



1 **Isotopic signatures of methane emission from oil**
2 **and natural gas plants in southwestern China**

3 Dingxi Chen^{1†}, Yi Liu^{2†}, Zetong Niu¹, Ao Wang¹, Pius Otwil¹, Yuanyuan Huang¹,
4 Zhongcong Sun¹, Xiaobing Pang³, Liyang Zhan⁴, Longfei Yu^{1*}

5 ¹Shenzhen Key Laboratory of Ecological Remediation and Carbon Sequestration,
6 Institute of Environment and Ecology, Tsinghua Shenzhen International Graduate
7 School, Tsinghua University, Shenzhen 518055, China

8 ²Safety, Environment and Technology Supervision Research Institute of PetroChina
9 Southwest Oil and Gas Field Company, Chengdu 610041, China

10 ³College of Environment, Zhejiang University of Technology, Hangzhou, 310014,
11 China

12 ⁴key Laboratory of Global Change and Marine-Atmospheric Chemistry, Third
13 Institute of Oceanography, Ministry of Natural Resources, Xiamen, 361005, China

14

15 *Corresponding authors: longfei.yu@sz.tsinghua.edu.cn

16 †These authors contributed equally.

17

18



19 **Abstract**

20 Methane (CH₄) emissions to atmosphere from Chinese oil and gas (ONG) sector are
21 subject to considerable uncertainty. The isotopic composition of CH₄ isotopes ($\delta^{13}\text{C}$)
22 varies between emission sources, enabling the identification of changes in specific CH₄
23 sources. However, there are few relevant studies in China, especially at the ONG site
24 level. We obtained CH₄ mixing ratios and isotopes from atmospheric samples collected
25 by UAV and ground monitoring, and employed the HYSPLIT model to investigate CH₄
26 distribution at ONG sites in southwest China. It was found that the CH₄ isotopic
27 signatures provide a strong basis for the emission intensity at the ONG sites. The
28 meteorological and site conditions were identified as the most influential factors in CH₄
29 distribution at sites. The CH₄ from the equipment area contributed approximately a
30 quarter of the CH₄ observed over the sites. The CH₄ source isotopic signatures ($\delta^{13}\text{C}$)
31 of this study were heavier than those globally, indicating that they were mainly
32 thermogenic sources. Finally, the heavier $\delta^{13}\text{C}$ of this region may lead to an
33 overestimation emission of global CH₄ from fossil fuel sources by 3.47 Tg CH₄ yr⁻¹,
34 and underestimation from microbial sources. This study highlights the importance of
35 regional CH₄ isotopes, with great significance for CH₄ inventories of global sectors.



1 Introduction

Methane (CH_4) is a major greenhouse gas (GHG) in the atmosphere, possessing a global warming potential 82.5 times greater than carbon dioxide (CO_2) over a 20-year timeline, and 29.8 times greater over a 100-year period (Ipcc, 2021). The mixing ratios of CH_4 in the atmosphere has increased by 150% since the industrial revolution, primarily driven by human activities (Hmiel et al., 2020; Saunois et al., 2016b; Tian et al., 2016; Skeie et al., 2023). The oil and natural gas (ONG) industry is one of the major contributors to anthropogenic CH_4 emissions accounting for approximately 25% of global emissions. Over the past 20 years, CH_4 emissions from the ONG industry have increased by about 23.1%, corresponding to an average annual growth rate of 1.1% (Lauvaux et al., 2022). However, some studies suggest that CH_4 emissions from fossil fuel sources are likely to be seriously underestimated (Lauvaux et al., 2022; Hmiel et al., 2020). In China, CH_4 emissions from ONG industry have been estimated to increase from 116.6 Gg in 1990 to 1124.8 Gg in 2018 (Epa, 2019), but various nationwide investigations tend to be highly variable and uncertain (Zhang et al., 2014) (Sun et al., 2022). Such discrepancy primarily arises from the scarcity of publicly available data and the accuracy of emission factors. The emission factor (EF) data used mainly come from the IPCC and its improvements, which may not accurately reflect the actual situation in China (Gao et al., 2022).

Overall, the general consensus is that the global CH_4 mixing ratios have been increasing over the past few decades (Schwietzke et al., 2016; Montzka et al., 2011; National Oceanic & Atmospheric Administration, 2024a). At present, the main controversy is the contribution sources of CH_4 (the drivers of the atmospheric CH_4 growth) and the high uncertainty of contribution (the uncertainty in CH_4 budget) (Kirschke et al., 2013; Saunois et al., 2016a; Rice et al., 2016; Tibrewal et al., 2024). The identification of CH_4 sources is essential for the estimating and reduction of CH_4 emissions.

The anthropogenic sources CH_4 accounting for about 50-65% of global CH_4 emissions come from human activities, including ONG industry, wetlands, agriculture



(e.g., ruminants, rice cultivation), landfills, and wastewater. However, the contribution of each CH₄ source is highly uncertain(Skeie et al., 2023). The presence of greenhouse gases is attributed to a multitude of sources. These sources exhibit distinct isotopic signatures, which serve as a valuable tool for the identification and differentiation of their origins(Schwietzke et al., 2016). Stable isotope is one of the common tools to distinguish different sources of the same substance(Suzuki, 2021; Peng et al., 2024; Leitner et al., 2020; Basu et al., 2022). A number of isotope pool mixing-models have been developed to quantify source contributions(Parnell et al., 2013)(Barthold et al., 2011), providing important constraints on the role of various anthropogenic and natural emissions to the overall greenhouse gas burden, and thereby enhancing our understanding of the complex dynamics of climate change(Zhang et al., 2022; Rigby et al., 2017). Several studies have attempted to use CH₄ isotopes for unraveling regional CH₄ emission patterns. Using the characteristics of carbon ($\delta^{13}\text{C}$) and hydrogen (δD) stable isotopic of CH₄, help distinguish between specific emitters of CH₄ from the Condamine region, Queensland, Australia (main CH₄ sources include coal seam gas related, piggery, ground and river seeps, feedlot and grazing cattle, landfill and others), the $\delta^{13}\text{C}$ and δD signatures of each CH₄ source were analyzed(Lu et al., 2021). Some researchers combined $\delta^{13}\text{C}$ with other models to separate industrial CH₄ emission sources from atmospheric(Assan et al., 2018). A recent research indicated that 85% CH₄ emissions growth from microbial sources during the period 2007 to 2016 were estimated based on $\delta^{13}\text{C}$ of CH₄ in the atmosphere(Basu et al., 2022). A study based on atmospheric $\delta^{13}\text{C}$ of CH₄ data showed that CH₄ emissions from the fossil fuel sector remained largely unchanged at the 1980s and 1990s levels, but increased significantly between 2000 and 2009(Rice et al., 2016). By analyzing $\delta^{13}\text{C}$ of CH₄, researchers suggested that a reduction in microbial CH₄ emissions in the Northern Hemisphere may have contributed to the stabilization of atmospheric CH₄ over the Millennium(Kai et al., 2011).

Global observations and researches on CH₄ source isotopic signatures from the ONG industry have been carried out and some results obtained, such as a global database of CH₄ isotopes from fossil fuels in the atmosphere has been established, according to the



95 latest research results to update timely(Schwietzke et al., 2016). Other studies have been
96 initiated at regional and urban scales, such as estimating CH₄ emissions from
97 abandoned ONG wells in the United States, and $\delta^{13}\text{C}$ of CH₄ has been employed to
98 distinguish the coalbed and nature gas sources(Townsend-Small et al., 2016). Another
99 research also reported the CH₄ isotopic signatures of ONG fields in Romania,
100 confirmed CH₄ in the region mainly from the ONG sector, and simultaneous resulted a
101 wide range of $\delta^{13}\text{C}$ values, which indicated regional variation in CH₄ isotopes(Menoud
102 et al., 2022). Recent advancements in UAV technology have facilitated novel
103 approaches to monitor and quantify CH₄ emissions, particularly in localized
104 settings(Shaw et al., 2021). For example, the airborne platform was used to monitor the
105 CH₄ emission from UK and Dutch offshore ONG installations, to quantify and identify
106 the sources(France et al., 2021), and UAV-based sampling systems were used to analyze
107 greenhouse gas stable isotope(Leitner et al., 2023). Nevertheless, the relevant studies
108 were largely concentrated in foreign countries, and a few reports have revealed the CH₄
109 isotopic values from Chinese ONG production regions (SI, Table S1). To date, no
110 research has examined the site-specific isotopic signatures of CH₄ emissions within the
111 industrial site in China. In addition, the CH₄ isotopic signatures at the site level is
112 regulated by many factors, such as source types(Zhang and Zhu, 2008; Schoell, 1980;
113 Liu et al., 2019), processing (e.g., purification or production of light hydrocarbon),
114 meteorological condition, sampling method, size of the site and so on. Therefore, the
115 isotope tools are likely to provide quantitative or semi-quantitative reference for
116 investigating regional or site-level CH₄ emission hotspots.

117 In order to fulfill for the lack of site-level CH₄ emission research, this study aims to
118 delineate the isotopic traits of CH₄ emitted from Chinese ONG industry stations, by
119 analyzing the sources of CH₄, and judging whether there is CH₄ emission in the field
120 stations combined with other information. Simultaneously, the database of CH₄ isotopes
121 in China will be enriched. We conducted monitoring and sampling of CH₄ at 11 ONG
122 sites in the central Sichuan Basin, China. We characterized the sources and isotopic
123 signatures of CH₄ based on isotope data derived from these samples. This study's data
124 significantly augments the CH₄ isotope database for ONG source in the central Sichuan



125 Basin, effectively bridging the previously existing gaps in both surface and upper
126 atmospheric CH₄ isotope data for these sites. Looking ahead, this expanded dataset will
127 serve as a foundational resource for future research, enabling more comprehensive
128 assessments of global CH₄ emissions and their sources, and potentially guiding the
129 development of targeted mitigation strategies for the ONG industry.



130 **2 Method**

131 **2.1 Study sites**

132 The study area is located in Sichuan Basin, Southwest China, where about 19 %
133 of the country's total natural gas reserves have been discovered(The People's
134 Government of Sichuan Province, 2024). Until 2022, the region has about 77,000 km
135 gas pipelines(National Bureau of Statistics, 2024). Between 2013 and2023, natural gas
136 production in this region increased from 21.31×10^9 to 59.48×10^9 m³(Sichuan
137 Provincial Bureau of Statistics, 2024), with an average annual growth rate of about 11%.
138 In 2020, ONG production in Sichuan accounted for 24% of China's total ONG
139 production (National Bureau of Statistics, 2024). We monitored CH₄ mixing ratios and
140 sampled air for isotope measurements across 11 ONG processing or transportation
141 stations in the central Sichuan Basin. The study region is characterized by a humid
142 subtropical climate, with consistently warm and humid conditions throughout the year.
143 The areas of these stations vary from 2,000 to 300,000 m², while the production
144 activities also vary, including natural gas purification plants, gas gathering stations,
145 light hydrocarbon plants, pigging stations, pressurization stations, etc. (Table 1). Most
146 of the ONG stations are located in rural areas, surrounded by mountains, forests,
147 farmlands, and reservoirs, and there are rivers located in the vicinity of only several
148 sites. Paddy fields are the main farmland in this area, and rice is the main grain
149 crop(Sichuan Provincial Department of Agriculture and Rural Affairs, 2024). For
150 reasons of privacy and confidentiality, the specific locations and contours of the ONG
151 stations cannot be disclosed in this paper.



Table 1 Background information of the studied production/processing sites for oil and natural gas

Site	Type	Area (m ²)	Processing capacity (10 ⁴ m ³ /d)	Surrounding environment	Activity
MX (S1)	Purification plant	25000	445	Forests, farmland	Natural gas processing, including membrane separation, adsorption, desulfurization, dehydration and other processes
SN (S2)		113000	3000	Forests, farmland, many ponds	
DQ (S5)	Gas gathering stations	5096	115	Forests, reservoirs	Gas Collection and transportation
XBQ (S3)		9420	278	Forests, farmland	
XQ (S4)		4220	1000	Farmland, ponds	
QTCSN (S7)	Light hydrocarbon plant	6650	10	Forests, farmland	C ³⁺ component of natural gas was recovered by low temperature separation process
QTCSZ (S8)		25257	30	Forests	
LHZ (S9)	Union Station	7958	2700	River	ONG centralized treatment, sewage treatment, product output
ZYZ (S11)	Supercharging station	7740	24	Farmland, ponds	Pressure and transmission
L1 (S10)	Central well station	8679	90.3	Forests, farmland, ponds	Gas Collection and transportation
XM (S6)	Pigging station	5167	630	River	

154

155 2.2 Sampling methods

156 From 13 April to 19 April 2023, we monitored and collected samples at 11 ONG
 157 production stations in the central Sichuan Basin, obtaining a total of 74 samples,
 158 including 28 ground samples and 46 air samples. Ground samples were collected at
 159 heights ranging from -0.5 m (0.5 m under the ground) to 2 m. Sampling locations were



160 chosen in open areas of each station, including areas near pipelines and production
161 equipment. Sampling in the area of pipelines and production equipment was performed
162 at locations that show abnormal mixing ratios after ground monitoring, and in instances
163 where no apparent CH₄ emission was detected, sampling was performed in the center
164 of the pipelines and production equipment area. For large field stations ($> 10,000 \text{ m}^2$),
165 multiple sampling points were established, while for small field stations ($< 10,000 \text{ m}^2$),
166 1-2 sampling points were established in facility areas, and the sampling time for each
167 sample was about 45-50 seconds. The drone was launched in open positions. Air
168 sampling was performed by an Unmanned Aerial Vehicle (UAV) equipped with an
169 automatic sampling pump (Fig. 1). The UAV model was a DJI-T10 upgraded version,
170 and the sampling pump model was KVP04-1.1-12V (1.25 L/min). Taking into account
171 the altitude ranges utilized in previous studies (Kim et al., 2025; Han et al., 2024; Chen
172 et al., 2024; Liu et al., 2021; Liu, 2018; Ali et al., 2017), along with the drone's flight
173 endurance and sampling duration, the monitoring altitude for this study is defined,
174 sampling heights were 50 m, 100 m, 200 m and 300 m respectively. Initially, a ground
175 sampling site was identified, typically within the pipeline vicinity of the plant.
176 Subsequently, a UAV equipped with an automatic sampling pump and air collection
177 bags was lifted to altitude of 300 m above the ground sampling site. The UAV then
178 sequentially descended to altitudes of 200, 100, and 50 m, respectively, dedicating 45
179 to 60 seconds at each elevation for collecting air samples. This systematic approach
180 ensures a comprehensive and stratified sampling strategy, facilitating the assessment of
181 atmospheric constituents at varying heights. The volume of each air sample was
182 approximately 1 L. All sites sampled at altitude, with the exception of S1, which
183 sampled at 200 m and 300 m, all other stations sampled at various altitudes. Air
184 sampling and UAV cruising were synchronized. HOONPO Teflon gas bags (1L, 2L
185 specifications) were used for gas sampling. In addition, we sampled the region near an
186 urban park and river to analyze the region's atmospheric CH₄ mixing ratio and isotope
187 information, collecting a total of 4 samples (2 from the riverbank, 2 from the park). We
188 also sampled a production well (built in the 1980s) that was out of repair and had
189 significant emissions, and the result was used as a reference for source signal analysis,



190 with a total of 3 samples collected (one from the open area of the site and two from the
191 leak). The sample list and test results are provided in (SI, Table S2).



192



193

194 **Fig. 1** UAV, automatic sampling system and sampling over the site.

195

196 The influence of meteorological conditions on the CH₄ mixing ratio and isotopes at
197 the field station was also considered. Therefore, a portable meteorological station was
198 deployed at each station during the sampling or monitoring periods. It was equipped
199 with a three-dimensional ultrasonic wind speed and direction sensor (model: M307200),
200 which recorded the wind speed (horizontal and vertical) and direction (horizontal and
201 vertical) near the ground (3 to 10 m according to field conditions), the sampling
202 frequency is 32 Hz with a resolution of 0.1 m/s for wind speed and 0.1° for wind
203 direction, and the accuracy of wind direction and speed is 2° and 0.2 m/s, respectively.
204 We also obtained air pressure, solar radiation, temperature, and relative humidity from
205 weather stations. Since the meteorological conditions at high altitudes (50 to 300 m)
206 cannot be monitored by instruments, we used the HYSPLIT model to test the influence
207 of wind speed and direction on our measurements of CH₄ mixing ratios and isotopes at



208 high altitudes.

209 **2.3 Measurement methods**

210 Gas samples were analyzed within one month after on-site sampling. Picarro G2132-
211 i was used to detect the isotope and mixing ratio of CH₄, which is based on unique
212 Cavity Ring-Down Spectroscopy (CRDS). The δ¹³C detection accuracy (1-σ, 1-hour
213 window) of the instrument is as follows: when the mixing ratio of CH₄ is greater than
214 1.8 ppm, the accuracy of 5-minute mean value is less than 0.8‰, when the mixing ratio
215 of CH₄ exceeds 10 ppm, the accuracy is less than 0.4‰(Picarro, 2024). The calibration
216 of the instrument was performed with CH₄ isotope standard gas (2.8 ppm, -68.6±0.3‰),
217 produced by Airgas company, USA. Standard gas measurements were performed daily,
218 before and after the start of the sample test, to correct the same-day test data (the
219 correction parameters of CH₄ isotope and mixing ratio were approximately 1.5‰ and
220 0 ppm, respectively). Each gas bag sample underwent three repeatedly measurements,
221 totaling 74 samples. For each sample measurement, analysis over 180 seconds was
222 performed on the Picarro G2132-i CRDS, and the average of the last 120 seconds of
223 CH₄ isotope and mixing ratio data was recorded as the sample assay value. Both CH₄
224 isotope and mixing ratio data are available for each test.

225

226 **2.4 Calculation of source isotopic signatures**

227 Based on the sample detection data, the method of Keeling plot method was used to
228 determine the CH₄ source(Keeling, 1958; Pataki et al., 2003) for each field station, as
229 shown in formula (1):

$$230 \quad \delta_{(a)} = [\text{CH}_{4(b)}] \cdot (\delta_{(b)} - \delta_{(s)}) \cdot 1/[\text{CH}_{4(a)}] + \delta_{(s)} \quad (1)$$

231 Where δ_(a), δ_(b), and δ_(s) represent the δ¹³C values of the sample, the background air
232 and the average source, respectively. [CH_{4(a)}] and [CH_{4(b)}] represent the CH₄ mole
233 fractions of the sample and the background air, respectively. The intercept (δ_(s)) of the
234 fit line is the isotope value of the CH₄ source present in the mixed sample. In linear
235 regression, 1/[CH_{4(a)}] and δ_(a) represent independent (X-axis) and dependent (Y-axis)
236 variables, respectively. This method is suitable for carbon dioxide, methane(Thom et
237 al., 1993), water vapor(Moreira et al., 1997), and other gases, but each gas has its



specific considerations (Pataki et al., 2003). The gas samples from each station were collected within 30 minutes, during which the atmospheric background values (isotope and mole fraction of CH₄) did not change, fulfilling the application conditions of this method (Lu et al., 2021).

2.5 HYSPLIT model

The Hybrid Single-Particle Lagrange Integrated Trajectory (HYSPLIT) model developed by the National Oceanic and Atmospheric Administration (NOAA) Air Resources Laboratory, is a widely used public platform for different atmospheric scales and supports online modules (Pereira et al., 2019; National Oceanic & Atmospheric Administration, 2024b). The model has been used to calculate the air mass transfer trajectories at different altitudes (Shan et al., 2009; McGowan and Clark, 2008; Stein et al., 2015). Examples of applications include meteorological analysis of ozone events (Shan et al., 2009), dust transport pathways (McGowan and Clark, 2008), dust storm simulation (Broomandi et al., 2017; Ashrafi et al., 2014), prediction of size distribution and mixing ratios of heavy metals in atmospheric aerosols (Chen et al., 2013) and so on. To analyze the influence of meteorological conditions on CH₄ mixing ratios and isotopes above the field station, wind direction and speed at different heights are required, which are available from the HYSPLIT model. The time resolution of the model could reach 1 hour and the height resolution was 1 meter. Backward trajectories were used in this study, to calculate 24-hour backward trajectories at ground, 50 m, 100 m, 200 m, and 300 m heights over each site, respectively. The input data included the longitude and latitude of the site from field measurements and sampling time, while the output information were wind direction and speed at different heights.

2.6 Source partitioning with end-member mixing method

End-member mixing method is a common method for identifying and quantifying major sources of runoff. Several solutes have been used as tracers (typically 2-6) to determine the contribution of each water source to total runoff. The method is based on the mass balance of water and tracer, and the following assumptions: (1) the water



268 solute is constant, (2) the tracer is conservative, (3) and the source solution has an
269 extreme concentration(Bugaets et al., 2023; Barthold et al., 2011). Here, we applied it
270 to gases, using CH₄ mixing ratios and isotopes as tracers to investigate the contribution
271 of atmospheric background, open surface area, and facility area to high-altitude CH₄.

272

273 **2.7 Statistics**

274 Data analysis and graphing were performed using Origin 2024 software for Windows.
275 Linear fitting was based on the principle of the Least square method, indicating the 0.95
276 confidence intervals. A value of $P < 0.05$ was considered significant for statistical
277 analysis, and the fitting results are expressed as fitting mean and standard deviation.
278 Maximum, minimum, mean, median, outliers, and 25% -75% range values were also
279 analyzed and reported in the figures or tables.



3 Results

3.1 Measurements of CH₄ mixing ratios and isotopes

The CH₄ mixing ratios and $\delta^{13}\text{C}$ -CH₄ values from the 11 stations in this study area ranged from 1.88 to 3.66 ppm and from -48.45‰ to -30.97‰, respectively. The maximum and minimum values of CH₄ isotopes were obtained at sites S2 and S6 (H: 200 m), respectively. The variation of the CH₄ mixing ratio and isotopic values at stations S2, S4, and S7 is significantly greater than that observed at other stations (Fig. 2). The CH₄ isotope and mixing ratio of the urban samples were $-46.45 \pm 0.49\text{‰}$ and 2.04 ± 0.07 ppm, respectively. The result of direct emissions from the production well was $-15.4 \pm 5.72\text{‰}$ and 118.98 ± 0.52 ppm, respectively (SI, Table S2). The range of ground CH₄ isotopic values observed at the field stations in the study area was -47.98‰ to -15.40‰, with an average of $-42.96 \pm 6.87\text{‰}$. The CH₄ mixing ratio and isotopic values in the production equipment areas of the majority of sites were higher than those in the open areas. However, there were exceptions, with some field stations displaying similar values (for example, S6 and S9). The range of air CH₄ isotopic values of the sites in the study area was -48.45 to -44.28‰, with an average value of $-46.43 \pm 1.08\text{‰}$. The ground measurements showed higher CH₄ mixing ratios and isotopic values than the air, which could be an indication of CH₄ emissions from ONG sites (Fig. 3).

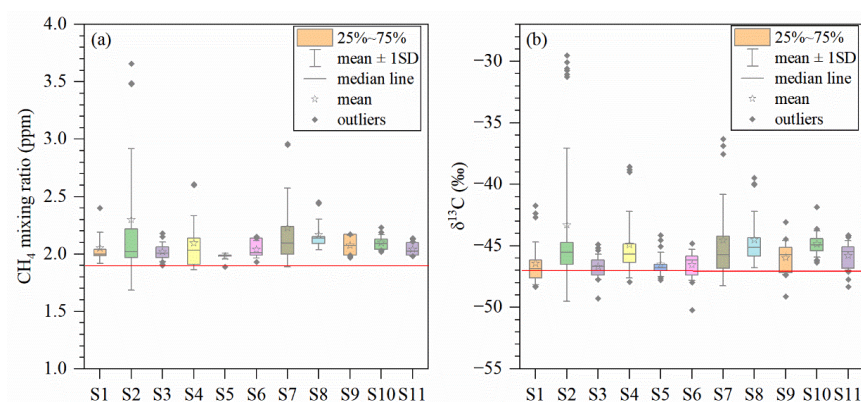


Fig. 2 Box whisker plots of CH₄ mixing ratios (a) and isotopic values (b) from the studied sites (mean, median, outliers, 25% -75% range, and 1 SD are indicated in the figures; the red lines refer to CH₄ mixing ratios (a, 1.9 ppm) and isotopic values (b, -47‰) from the atmospheric background.

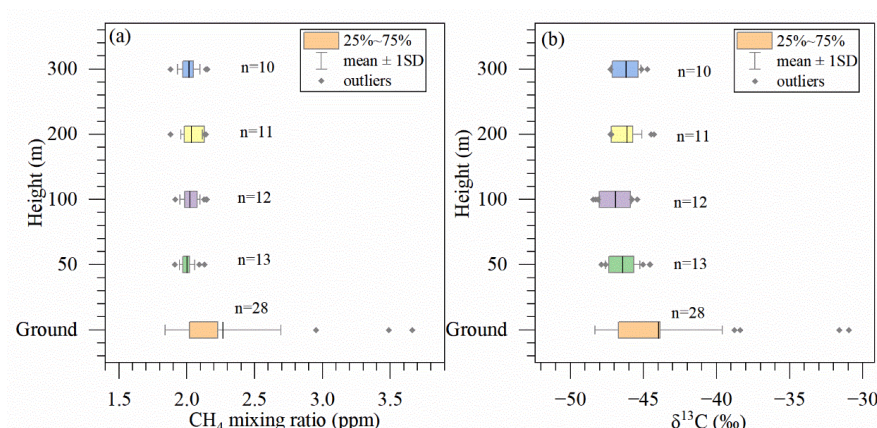


Fig. 3 Box whisker plots showing the variations of CH₄ mixing ratios (a) and isotopic values (b) at different heights (from ground to 300 m at all sites); include mean, 25% - 75% range, and 1 SD; “n” represents the number of samples.

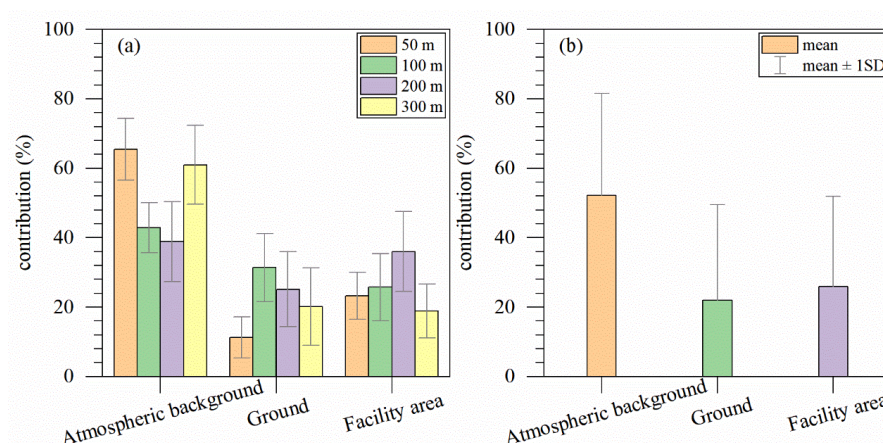
3.2 Vertical profiles of CH₄ mixing ratios and isotopes and source partitioning

The distributional trend of the CH₄ mixing ratios and isotopes in the vertical direction differed. For instance, the mean CH₄ mixing ratios were higher at 100 m than at 50 m, yet the isotopic values (δ¹³C) were lower (Fig. 3). From the perspective of a single station, the conditions were similar yet more complex. Some stations exhibited consistent trends (S1, S3, S6, S7, S9, S11), while others displayed different trends (S2, S4, S5, S8, S10) (SI, Fig. S1). For instance, the CH₄ mixing ratio and isotopic values at 100 m and 200 m altitude of station S8 were inversely proportional. As the altitude increased from the ground to 300 m, the CH₄ isotopic values of stations S4 and S1 exhibited a decline, ranging from -45.10‰ to -47.27‰ (ground to 300 m) and from -42.27‰ to -47.92‰ (ground to 100 m), respectively (SI, Fig. S1). The CH₄ isotopic values of stations S3 and S6 initially decreased with increasing altitude and subsequently increased, reaching a minimum at 100 m altitude (-48.45‰ and -48.11‰, respectively). The variation of the CH₄ isotope vertical profile at station S8 was analogous to that observed at sites S6 and S3, with the exception that the CH₄ isotopic minimum value reached -46.18‰ at 200 m altitude. The variation of CH₄ isotopic values with altitude at station S9 was complex, exhibiting a decrease followed by an increase, which then decreased again, reaching minimum and maximum values at 50 m



326 (-45.06‰) and 200 m (-44.47‰), respectively.

327 The end-member mixing method is a commonly employed technique for calculating
328 isotope mixing by various sources of GHGs (Bugaut et al., 2023). In this study, we
329 determined the contribution of CH₄ from the atmospheric background, surface, and
330 facility areas to the air over the sites (the details and results are presented in SI part 1).
331 The results demonstrated that the atmospheric background contributed $52.2 \pm 28.9\%$ to
332 the total, the facility area contributed $21.9 \pm 27.1\%$, and the ground open area
333 contributed $25.9 \pm 25.5\%$ (Fig. 4b). The contribution of the atmospheric background
334 initially decreased and then increased, reaching a minimum at 200 m, while the
335 contribution of the ground and facility areas initially increased and then decreased,
336 reaching a maximum at 100 m and 200 m, respectively (Fig. 4a). In cases where
337 calculations are not feasible, the CH₄ emissions may be predominantly influenced by
338 microbial activity or other local sources in the vicinity of the sites.



339

340 **Fig. 4** The fractional contributions from ambient background, surface, and facility areas
341 contribute to the vertical atmospheric sampling. (a) the proportion of contributions to
342 different heights with standard error; (b) the proportion of contributions to all heights
343 of all stations with 1SD.

344

345 3.3 Characteristics of source isotopes

346 The Keeling plot method was employed to determine the isotopic signatures ($\delta^{13}\text{C}$)
347 of CH₄ sources at each station, with the results presented in Fig. 5. The range of the
348 CH₄ source isotopic signatures varied from $-50.7 \pm 8.7\text{‰}$ to $-10.9 \pm 5.5\text{‰}$, indicating



349 that they were mainly thermogenic sources (associated with oil production)(Menoud et
350 al., 2022; Sherwood Lollar et al., 2002). The value of the CH₄ source signature for
351 station S10 was $-50.7\text{‰} \pm 8.7\text{‰}$, which was lower than the atmospheric background
352 value. Additionally, the data fitting for this field station was poor ($R^2 = 0.03$). This may
353 be attributed to the low CH₄ emissions from the site and the primary contribution of
354 CH₄ from microbial sources in the surrounding area (Table 1). Furthermore, the
355 measurements of the CH₄ samples collected in urban parks and riverside revealed that
356 the CH₄ source signature value was $-35.1\text{‰} \pm 6.3\text{‰}$, which was considerably higher
357 than the atmospheric background value. It is yet to be determined whether this value
358 can be considered representative of the atmospheric background value of the study area.
359 Additional sample data are necessary to facilitate a more comprehensive analysis. On
360 the other hand, the direct measurements of emission from wells indicated that source
361 ¹³C signature was $-18.7 \pm 6.3\text{‰}$, which is close to the result of the sample test ($-15.4 \pm$
362 5.72‰) (SI, Table S2). Globally, the range of CH₄ isotopic values from fossil fuels is -
363 75‰ to -25‰ , with a median value of -44‰ (Defrattyka et al., 2021). Our results fall
364 outside this range and exhibit higher values.



4 Discussion

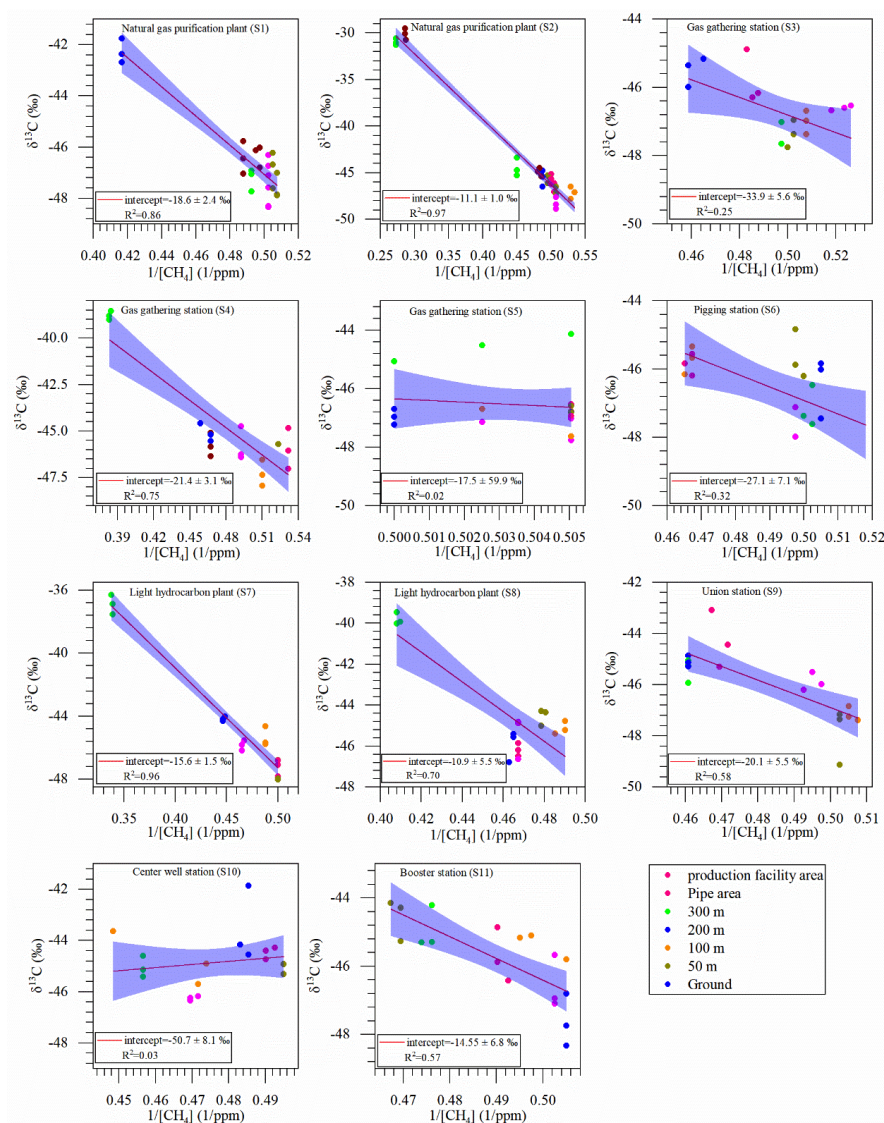
4.1 Variations of CH₄ isotopic values from the atmosphere and ground

The mean values of CH₄ isotope were higher than the atmospheric background ($-47.0 \pm 0.3\text{‰}$) at all sites (Tyler, 1986), with some sites exhibiting values close to the atmospheric background (e.g., S1, S3, and S5). However, the average values of CH₄ mixing ratios were significantly higher than the atmospheric background (1.9 ppm) at all stations (Skeie et al., 2023). This indicated that CH₄ emissions occurred at all sites, with obvious leakage at most stations. On the other hand, the correlation between CH₄ mixing ratios and isotopes at the ONG sites was significant ($R^2=0.90$). Besides, the ground exhibited a stronger correlation ($R^2=0.94$) than the air ($R^2=0.31$) (SI, Fig. S2). These findings indicated that the CH₄ sources in the surface of the station were rather similar and derived from the ONG industry, and that CH₄ in the region has a similar genesis. This conclusion was further supported by the analogous CH₄ source isotopic signatures from most stations determined by keeling plot approach (Fig. 5). In addition, an investigation of the potential sources of CH₄ in the vicinity of the ONG sites revealed that the primary source of CH₄ at the station was from ONG, with other sources exerting a lesser impact.

However, multiple sources may be involved when looking into the relationship between mixing ratios and isotopes at each site alone (Fig. 5). The hypothesis was corroborated by isotope data. We discovered that approximately half of the ONG production stations (6 out of 11) exhibited higher ground CH₄ isotopic values ($\delta^{13}\text{C}$) than those observed in the air (S1, S3, S4, S7, S8, S10). The observed decline in isotope values can be attributed to the mixing of microbial sources of CH₄ present in the vicinity of the stations. Conversely, the remaining half of the stations (5 out of 11) displayed ground CH₄ isotopes that were either lower than or comparable to those observed in the air (S2, S5, S6, S9, S11). This discrepancy may be attributed to the uncertainty associated with the sources of CH₄ in the air, which is more sensitive to meteorological conditions. Additionally, the majority of sites exhibit elevated CH₄ mixing ratios and isotopic signatures in their pipeline and facility areas. Studies have indicated that infrastructure, including components such as dehydrators, valves, compressors, and



395 pipelines, represents a significant source of CH₄ emissions from the ONG system.
396 Infrastructure is particularly vulnerable to CH₄ leakage due to corrosion and
397 wear (Anifowose et al., 2014; Fernandez et al., 2005; Burnham et al., 2012; Anifowose
398 and Odubela, 2015).



399 **Fig. 5** The CH₄ source isotopic signatures of 11 field stations. The blue area represents
400 the 95% confidence interval, and the red line is the result of linear regression posterior
401 mean fit; The samples in different positions are distinguished by different colors. The
402 intercept and R^2 are given, which means the source isotope signal value and the fitting
403



404 degree, respectively.

405

406 **4.2 Factors of drone-based isotope measurements in the atmosphere**

407 Significant variability was evident in the CH₄ mixing ratios and isotopic signatures
408 at the stations, with notable discrepancies observed at varying altitudes. This
409 inconsistency is likely attributable to a number of factors, including the presence of
410 additional CH₄ sources in the vicinity and the influence of meteorological
411 conditions (Kavitha and Nair, 2016). An examination of the site's environment revealed
412 that the area was predominantly forested, with agricultural land (paddy fields), water
413 bodies, and human settlements also present. Paddy fields and ponds have been
414 identified as the primary microbial sources of CH₄, characterized by lighter
415 isotopes (Minami and Neue, 1994; Wang et al., 2023; Vizza et al., 2022). The influence
416 of meteorological conditions is significant and complex, and challenging to analyze.
417 Wind direction and speed were obtained using the HYSPLIT model to assist with the
418 analysis (due to privacy considerations, the specific locations cannot be disclosed in
419 this work, only the data can be provided, SI, Table S3). Integration of the HYSPLIT
420 model data with that obtained from the meteorological station indicates that the results
421 produced by HYSPLIT were credible (SI, Fig. S3). The correlation analysis between
422 wind speed and CH₄ isotope results revealed an exponential relationship with an R-
423 squared value of 0.33 (SI, Fig. S4). This indicates that as wind speed increases, the
424 impact of CH₄ diffusion and dilution becomes more significant. Wind direction plays a
425 role in the uncertainty of CH₄ distribution, as it has a significant influence on CH₄
426 transport near the surface, resulting in a non-uniform distribution of CH₄ and typically
427 higher mixing ratios downwind from the emission source. Furthermore, upwind CH₄
428 sources can have a notable impact on CH₄ levels over the station. The utilization of
429 HYSPLIT model serves a crucial function in this regard (SI, Fig. S5 for a detailed
430 example of S7 site). To illustrate, the presence of a large wetland upwind can result in
431 air masses transporting microbial CH₄, consequently affecting the CH₄ mixing ratios
432 and isotopes above the station.

433 Moreover, the conditions at the station are among the primary determinants of the



434 results, encompassing factors such as the size of the sites, the treatment processes
435 employed, the treatment capacity, and the timing and location of sampling. A larger site
436 is likely to produce a great quantity of CH₄ emissions(Omara et al., 2016) and
437 accumulate CH₄ from a wider area, thereby exerting a more significant influence on the
438 air's CH₄ content. A correlation was observed between the area and the isotopes. It is
439 noteworthy that the correlation is enhanced when the site area was less than 10,000 m²
440 (SI, Fig. S6). This may be attributed to the fact that larger site areas encompass a wider
441 array of factors, which can exert a more significant influence. By contrast, the treatment
442 processes that involve physical chemistry may exert isotope fractionation effects that
443 affect CH₄ isotopes ($\delta^{13}\text{C}$), and the general heavier isotopes of this study may be
444 influenced by the treatment processes. The intermittent nature of emissions from the
445 site facilities introduces an element of uncertainty with regard to the sampling time and
446 locations(Omara et al., 2016). The results of the Principal Component Analysis (PCA)
447 demonstrated a weak relationship among wind direction, wind speed and isotopes, and
448 a strong correlation between the size and capacity of the sites with CH₄ isotopes (SI,
449 Fig. S7).

450

451 **4.3 Global source isotopic signatures of ONG-derived CH₄**

452 Previous studies have investigated the characteristics of CH₄ isotopes in Chinese
453 ONG production regions, mainly in the Sichuan Basin, Xinjiang, Northeastern China,
454 and the Ordos Basin. Based on previous work, the reported values of CH₄ isotopes cover
455 a wide range, from -54.9‰ to -17.4‰ (SI, Table S1). In general, the origin of natural
456 gas can be divided into two major categories: biogenic and abiogenic gas(Sherwood
457 Lollar et al., 2002; Dai et al., 2005), of which biogenic gases include “coal-type” and
458 “oil-type” gases(Liu et al., 2019; Dai et al., 1985; Dai et al., 1992; Xu, 1994). Studies
459 have suggested that CH₄ of different origin carries distinct isotopic characteristics(Cai
460 et al., 2013; Huang et al., 2017; Wang et al., 2018; Zhang et al., 2018; Zou et al., 2007;
461 Zhu et al., 2014). This study is situated in the central region of the Sichuan Basin, where
462 previous research on CH₄ isotopes has predominantly concentrated on large-scale
463 statistical analyses. To date, no studies have specifically focused on the isotopic



464 characteristics of CH₄ emanating from ONG industrial sites in this area. The Sichuan
465 Basin has a complex geological environment and many gas-production layers, such as
466 Cambrian, Ordovician, Carboniferous, Jurassic, etc., and CH₄ from different layers with
467 various isotopic characteristics(Zhang et al., 2018; Cai et al., 2013). In comparison to
468 the findings of other researchers on CH₄ isotopes in the Sichuan Basin (SI, Table S1),
469 our results of ¹³C-CH₄ isotope signatures spanned more widely and also appeared to be
470 heavier. In another study, Menoud et al.(Menoud et al., 2022) examined isotopic
471 signatures of CH₄ from an ONG extraction plant in Romania. Their methodology aligns
472 closely with ours, and their findings indicate a range of $\delta^{13}\text{C}$ values from $-67.8 \pm 1.2 \%$
473 to $-22.4 \pm 0.04 \%$. Generally, our results showed heavier isotopes source signatures,
474 exceeding the global mean of fossil fuel CH₄ isotope ($-44.0 \pm 0.7\%$)(Schwietzke et al.,
475 2016). This discrepancy can be attributed to a number of factors, including geographical
476 differences(Menoud et al., 2022), the treatment processing of natural gas, and the size
477 of samples. A comparison of the CH₄ isotopic signatures from the global ONG
478 system(Menoud et al., 2022; Lopez et al., 2017; Hoheisel et al., 2019; Defratyka et al.,
479 2021; Kang et al., 2014; Jenden et al., 1993) is presented in Fig. 6. The $\delta^{13}\text{C}$ of CH₄
480 was found to be lighter in the United States and Canada, but heavier in China. Regional
481 variations in $\delta^{13}\text{C}$ values were observed, even within the same region, with fluctuations
482 occurring. Our results exhibited a significantly heavier $\delta^{13}\text{C}$ than those of other studies.
483 This was attributed to differences in the origin of CH₄, with geographical differences
484 playing a prominent role(Zhang and Zhu, 2008; Wang et al., 2018; Defratyka et al.,
485 2021; Schoell, 1980).

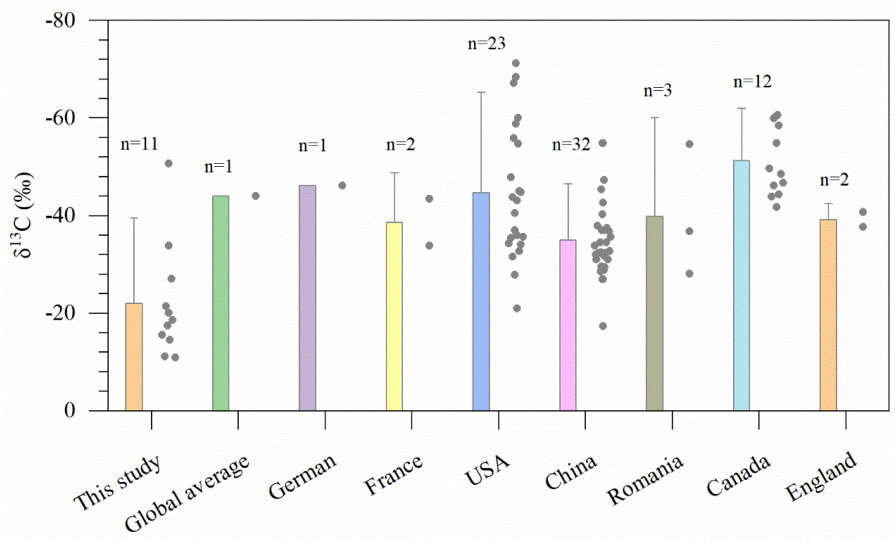


Fig. 6 An overview of global isotopic signals of CH₄ emitted from ONG industry or geo-thermal sources; data from both literature and this study are included. The right side of the box chart is the data point, the number of data points is also shown at the top of the box chart, and carry on the error analysis. “n” represents the number of data points.

The $\delta^{13}\text{C}$ of CH₄ represents a valuable indicator for constraining and estimating CH₄ emissions particularly from anthropogenic sources of the globe (Milkov et al., 2020). As a sum-up, the mean $\delta^{13}\text{C}$ signatures of CH₄ sources as indicated from measurements of atmospheric background integrated the collective contributions from various sources of CH₄ (SI, Fig. S8). Hence, with updated isotopic signatures for specific sources such as ONG industry, the previous conclusions on global contribution/flux of CH₄ from ONG industry may need to be revised (Schwietzke et al., 2016). In comparison with previous studies, the $\delta^{13}\text{C}$ values from ONG industry in our work (-21.95‰ based on 11 stations) are significantly higher, especially different from the global flux-weighted averaged by Schwietzke et al. (Schwietzke et al., 2016). By incorporation of flux contribution from Chinese ONG industry, isotope signatures as well as global datasets utilized in the previous work (Schwietzke et al., 2016), we conducted a sensitivity analysis, examining the effect on diverse source contributions (in flux) when updated the $\delta^{13}\text{C}$ -CH₄ from Chinese ONG industry (SI, part 2 for details). Our finding suggests



507 that, our field observation of isotope signature from China would elevate global fossil
508 fuel-derived CH₄ isotopes signature by about 0.5‰; as a consequence, the new result
509 would lead to a smaller contribution from global ONG industry (corresponds to an
510 overestimation of emissions by 3.47 Tg CH₄ yr⁻¹) but a larger contribution from
511 microbial sources. This findings is consistent with some recent research findings, such
512 as Chandra et al.(Chandra et al., 2024), who reported that CH₄ emissions decreased in
513 fossil fuel sources, while increasing in microbial sources during 1990-2020. In
514 Australia, CH₄ emissions from agricultural ponds (microbial sources) were
515 underestimated in national greenhouse gas inventories(Malerba et al., 2022). Overall,
516 the decline of global mean CH₄ isotopic signals seem to slightly speed up in recent
517 years, likely supporting the importance of microbial emissions. Previous studies have
518 identified potential avenues for reducing CH₄ leakage in the ONG industry, including
519 improvements in technology, equipment, and management practices(Us Environmental
520 Protection Agency, 2012; China National Petroleum Corporation, 2023), this may
521 provide an insight into the overestimation of CH₄ emissions from ONG sources.

522

523 **4.4 Feasibility and limitations**

524 Atmosphere CH₄ isotopic research has shown its power in distinguishing between
525 microbial and fossil sources of global atmospheric CH₄ trends(Basu et al., 2022;
526 Bruhwiler et al., 2017). However, due to scarcity of observational evidence of various
527 CH₄ source signatures, large uncertainties still exist for such estimations. The objective
528 of our research was to distinguish sources of CH₄ as well as to quantify CH₄ leakage
529 strength at site-level, providing basic but convincing data for constraining CH₄ sources.
530 With both ground- and air-based approaches, our study has demonstrated the feasibility
531 of our work in studying the characteristics of CH₄ sources and their influencing factors
532 at ONG stations in SW China. Nevertheless, it is necessary to point out, that the impact
533 of meteorological conditions and site conditions on the dampening/masking of CH₄
534 isotope signatures in the atmosphere may be significant. Therefore, the reconciliation
535 between ground and atmospheric measurements as well as source partitioning remain
536 to be further validated, given more sampling coverage both spatially and temporally. In



537 addition, more sampling at different locations or different ONG plants will be greatly
538 beneficial to the constraints on CH₄ source isotope signature from fossil fuel industry
539 in China.



540 **5 Summary**

541 The objective of this study is to differentiate CH₄ sources and examine the $\delta^{13}\text{C}$
542 isotopic characteristics at locations where gas samples were collected from ONG
543 stations in the central Sichuan Basin, China. The characteristics of CH₄ isotopes were
544 analyzed on the ground, in the air, and with regard to the vertical variations of CH₄
545 isotopes. Coupled with an analysis of the surrounding environment of the stations, we
546 reached the conclusion that the primary source of CH₄ at the ONG stations is emissions
547 from production facilities. Furthermore, CH₄ on the ground at the majority of sites is
548 more significantly influenced by the ONG source, while CH₄ in the air is more affected
549 by meteorological conditions. Additionally, the vertical variation of CH₄ isotopes is
550 complex and changeable, and is affected by several factors, including meteorological
551 conditions, station size, sample size, and other factors. The isotopic values of CH₄ from
552 various sites were also analyzed to determine the sources of the gas. The results showed
553 that the isotopic values of CH₄ from the ONG ranged from $-50.7 \pm 8.7\text{‰}$ to $-10.9 \pm$
554 5.5‰ , indicating a heavy $\delta^{13}\text{C}$ of fossil fuel. In comparison with the CH₄ source isotopic
555 values from the ONG globally, the results of this study revealed heavier isotopic
556 signatures. This study contributes to the global CH₄ isotope database from the ONG,
557 and addresses a gap in CH₄ isotope research at the site level in China. The primary
558 factors influencing the CH₄ isotope at field stations are the station's intrinsic
559 characteristics and the meteorological conditions present, as evidenced by the PCA
560 analysis. A weighted calculation on a global scale based on the results of this study
561 suggests that CH₄ emissions from microbial sources may be underestimated, while
562 those from fossil fuel sources may be overestimated. It is our contention that an
563 investigation into the isotopic characteristics of CH₄ at the site will prove invaluable in
564 distinguishing between the various sources of CH₄ and accounting for emissions.



565 **Acknowledgements**

566 This work was financially supported by the Scientific Research Start-up Funds
567 (QD2022010C) from Tsinghua Shenzhen International Graduate School and Cross-
568 disciplinary Research and Innovation Fund Research Plan (Grant No. JC2022010) from
569 Tsinghua Shenzhen International Graduate School. We are grateful to the kind support
570 from staff members in ONG plants from SW China.

571

572 **Author contributions**

573 D. Chen and Y. Liu conceptualized the study, with guidance from L. Yu. D. Chen and
574 Y. Liu conducted the field observation and sample analysis, with the help from Ze. Niu,
575 A. Wang and X. Pang. Y. Huang contributed data for the global literature analysis. D.
576 Chen, Y. Liu and L. Yu wrote the manuscript together. All coauthors reviewed and
577 contributed to the revision and finalization of the manuscript.

578

579 **Competing interests**

580 The authors declare no competing interests.

581

582 **Data availability**

583 All the data published in this work could be accessed upon request from the
584 corresponding author.



References

- Ali, H., Odeh, M., Odeh, A., Abou-ElNour, A. A., and Tarique, M.: Unmanned Aerial Vehicular System for Greenhouse Gas Measurement and Automatic Landing, *Netw. Protoc. Algorithms*, 9, 56-76, 2017.
- Anifowose, B. and Odubela, M.: Methane emissions from oil and gas transport facilities – exploring innovative ways to mitigate environmental consequences, *Journal of Cleaner Production*, 92, 121-133, 2015.
- Anifowose, B., Lawler, D., van der Horst, D., and Chapman, L.: Evaluating interdiction of oil pipelines at river crossings using Environmental Impact Assessments, *Area*, 46, 4-17, 2014.
- Ashrafi, K., Shafiepour-Motlagh, M., Aslemand, A., and Ghader, S.: Dust storm simulation over Iran using HYSPLIT, *Journal of environmental health science and engineering*, 12, 1-9, 2014.
- Assan, S., Vogel, F. R., Gros, V., Baudic, A., Staufer, J., and Ciais, P.: Can we separate industrial CH₄ emission sources from atmospheric observations? - A test case for carbon isotopes, PMF and enhanced APCA, *Atmospheric Environment*, 187, 317-327, 2018.
- Barthold, F. K., Tyralla, C., Schneider, K., Vaché, K. B., Frede, H.-G., and Breuer, L.: How many tracers do we need for end member mixing analysis (EMMA)? A sensitivity analysis, *Water Resources Research*, 47, 2011.
- Basu, S., Lan, X., Dlugokencky, E., Michel, S., Schwietzke, S., Miller, J. B., Bruhwiler, L., Oh, Y., Tans, P. P., and Apadula, F.: Estimating emissions of methane consistent with atmospheric measurements of methane and $\delta^{13}\text{C}$ of methane, *Atmospheric Chemistry and Physics Discussions*, 2022, 1-38, 2022.
- Broomandi, P., Dabir, B., Bonakdarpour, B., and Rashidi, Y.: Identification of the sources of dust storms in the City of Ahvaz by HYSPLIT, *Pollution*, 3, 341-348, 2017.
- Bruhwiler, L. M., Basu, S., Bergamaschi, P., Bousquet, P., Dlugokencky, E., Houweling, S., Ishizawa, M., Kim, H.-S., Locatelli, R., Maksyutov, S., Montzka, S., Pandey, S., Patra, P. K., Petron, G., Saunio, M., Sweeney, C., Schwietzke, S., Tans, P., and Weatherhead, E. C.: U.S. CH₄ emissions from oil and gas production: Have recent large increases been detected?, *Journal of Geophysical Research: Atmospheres*, 122, 4070-4083, 2017.
- Bugaets, A., Gartsman, B., Gubareva, T., Lupakov, S., Kalugin, A., Shamov, V., and Gonchukov, L.: Comparing the Runoff Decompositions of Small Experimental Catchments: End-Member Mixing Analysis (EMMA) vs. Hydrological Modelling, *Water*, 15, 752, 2023.
- Burnham, A., Han, J., Clark, C. E., Wang, M., Dunn, J. B., and Palou-Rivera, I.: Life-cycle greenhouse gas emissions of shale gas, natural gas, coal, and petroleum, *Environmental science & technology*, 46, 619-627, 2012.
- Cai, C., Zhang, C., He, H., and Tang, Y.: Carbon isotope fractionation during methane-dominated TSR in East Sichuan Basin gasfields, China: A review, *Marine and Petroleum Geology*, 48, 100-110, 2013.
- Chandra, N., Patra, P. K., Fujita, R., Höglund-Isaksson, L., Umezawa, T., Goto, D., Morimoto, S., Vaughn, B. H., and Röckmann, T.: Methane emissions decreased in fossil fuel exploitation and sustainably increased in microbial source sectors during 1990–2020, *Communications Earth & Environment*, 5, 147, 2024.
- Chen, B., Stein, A. F., Maldonado, P. G., Sanchez de la Campa, A. M., Gonzalez-Castanedo, Y., Castell, N., and de la Rosa, J. D.: Size distribution and concentrations of heavy metals in atmospheric



- 628 aerosols originating from industrial emissions as predicted by the HYSPLIT model, *Atmospheric*
629 *Environment*, 71, 234-244, 2013.
- 630 Chen, L., Pang, X., Wu, Z., Huang, R., Hu, J., Liu, Y., Zhou, L., Zhou, J., and Wang, Z.: Unmanned
631 aerial vehicles equipped with sensor packages to study spatiotemporal variations of air pollutants in
632 industry parks, *Philosophical Transactions of the Royal Society A: Mathematical, Physical and*
633 *Engineering Sciences*, 382, 20230314, doi:10.1098/rsta.2023.0314, 2024.
- 634 “Intelligent” control of methane emission by digital module in southwest oil and gas field:
635 <http://news.cnpc.com.cn/system/2023/12/22/030121011.shtml>, last
636 Dai, J., Pei, X., and Qi, H.: Natural gas geology in China, Petroleum Publication, 42-46, 1992.
- 637 Dai, J., Qi, H., and Song, Y.: Primary discussion of some parameters for identification of coal-and oil-
638 type gases, *Acta Petrolei Sinica*, 6, 31-38, 1985.
- 639 Dai, J., Yang, S., Chen, H., and Shen, X.: Geochemistry and occurrence of inorganic gas accumulations
640 in Chinese sedimentary basins, *Organic Geochemistry*, 36, 1664-1688, 2005.
- 641 Defratyka, S. M., Paris, J.-D., Yver-Kwok, C., Fernandez, J. M., Korben, P., and Bousquet, P.: Mapping
642 Urban Methane Sources in Paris, France, *Environmental Science & Technology*, 55, 8583-8591,
643 2021.
- 644 Non-CO₂ Greenhouse Gas Emission Projections & Mitigation: [https://www.epa.gov/global-mitigation-](https://www.epa.gov/global-mitigation-non-co2-greenhouse-gases)
645 [non-co₂-greenhouse-gases](https://www.epa.gov/global-mitigation-non-co2-greenhouse-gases), last
- 646 Fernandez, R., Petrusak, R., Robinson, D., and Zavadil, D.: Cost-Effective Methane Emissions
647 Reductions for Small and Midsize Natural Gas Producers, *Journal of Petroleum Technology*, 57, 34-
648 42, 2005.
- 649 France, J. L., Bateson, P., Dominutti, P., Allen, G., Andrews, S., Bauguitte, S., Coleman, M., Lachlan-
650 Cope, T., Fisher, R. E., and Huang, L.: Facility level measurement of offshore oil and gas
651 installations from a medium-sized airborne platform: method development for quantification and
652 source identification of methane emissions, *Atmospheric Measurement Techniques*, 14, 71-88, 2021.
- 653 Gao, J., Guan, C., and Zhang, B.: Why are methane emissions from China's oil & natural gas systems
654 still unclear? A review of current bottom-up inventories, *Science of The Total Environment*, 807,
655 151076, 2022.
- 656 Han, T., Xie, C., Yang, Y., Zhang, Y., Huang, Y., Liu, Y., Chen, K., Sun, H., Zhou, J., Liu, C., Guo, J.,
657 Wu, Z., and Li, S.-M.: Spatial mapping of greenhouse gases using a UAV monitoring platform over a
658 megacity in China, *Science of The Total Environment*, 951, 175428,
659 <https://doi.org/10.1016/j.scitotenv.2024.175428>, 2024.
- 660 Hmiel, B., Petrenko, V. V., Dyonisius, M. N., Buizert, C., Smith, A. M., Place, P. F., Harth, C.,
661 Beaudette, R., Hua, Q., Yang, B., Vimont, I., Michel, S. E., Severinghaus, J. P., Etheridge, D.,
662 Bromley, T., Schmitt, J., Faïn, X., Weiss, R. F., and Dlugokencky, E.: Preindustrial ¹⁴CH₄ indicates
663 greater anthropogenic fossil CH₄ emissions, *Nature*, 578, 409-412, 2020.
- 664 Hoheisel, A., Yeman, C., Dinger, F., Eckhardt, H., and Schmidt, M.: An improved method for mobile
665 characterisation of δ¹³CH₄ source signatures and its application in Germany, *Atmos. Meas. Tech.*,
666 12, 1123-1139, 2019.
- 667 Huang, S., Feng, Z., Gu, T., Gong, D., Peng, W., and Yuan, M.: Multiple origins of the Paleogene
668 natural gases and effects of secondary alteration in Liaohe Basin, northeast China: Insights from the
669 molecular and stable isotopic compositions, *International Journal of Coal Geology*, 172, 134-148,
670 2017.
- 671 IPCC: Climate Chang 2021 The Physical Science Basis, 1017, 2021.



- 672 Jenden, P. D., Drazan, D. J., and Kaplan, I. R.: Mixing of Thermogenic Natural Gases in Northern
673 Appalachian Basin1, AAPG Bulletin, 77, 980-998, 1993.
- 674 Kai, F. M., Tyler, S. C., Randerson, J. T., and Blake, D. R.: Reduced methane growth rate explained by
675 decreased Northern Hemisphere microbial sources, *Nature*, 476, 194-197, 2011.
- 676 Kang, M., Kanno, C. M., Reid, M. C., Zhang, X., Mauzerall, D. L., Celia, M. A., Chen, Y., and Onstott,
677 T. C.: Direct measurements of methane emissions from abandoned oil and gas wells in Pennsylvania,
678 *Proceedings of the National Academy of Sciences*, 111, 18173-18177, 2014.
- 679 Kavitha, M. and Nair, P. R.: Non-homogeneous vertical distribution of methane over Indian region
680 using surface, aircraft and satellite based data, *Atmospheric Environment*, 141, 174-185, 2016.
- 681 Keeling, C. D.: The concentration and isotopic abundances of atmospheric carbon dioxide in rural
682 areas, *Geochimica et Cosmochimica Acta*, 13, 322-334, 1958.
- 683 Kim, H., Kim, K. T., Jeong, S., Lee, Y. S., Zhao, X., and Kim, J. Y.: Enhancing Uncrewed Aerial
684 Vehicle Techniques for Monitoring Greenhouse Gas Plumes at Point Sources, *Atmospheric*
685 *Environment*, 342, 120924, <https://doi.org/10.1016/j.atmosenv.2024.120924>, 2025.
- 686 Kirschke, S., Bousquet, P., Ciais, P., Saunio, M., Canadell, J. G., Dlugokencky, E. J., Bergamaschi, P.,
687 Bergmann, D., Blake, D. R., Bruhwiler, L., Cameron-Smith, P., Castaldi, S., Chevallier, F., Feng, L.,
688 Fraser, A., Heimann, M., Hodson, E. L., Houweling, S., Josse, B., Fraser, P. J., Krummel, P. B.,
689 Lamarque, J.-F., Langenfelds, R. L., Le Quéré, C., Naik, V., O'Doherty, S., Palmer, P. I., Pison, I.,
690 Plummer, D., Poulter, B., Prinn, R. G., Rigby, M., Ringeval, B., Santini, M., Schmidt, M., Shindell,
691 D. T., Simpson, I. J., Spahni, R., Steele, L. P., Strode, S. A., Sudo, K., Szopa, S., van der Werf, G. R.,
692 Voulgarakis, A., van Weele, M., Weiss, R. F., Williams, J. E., and Zeng, G.: Three decades of global
693 methane sources and sinks, *Nature Geoscience*, 6, 813-823, 2013.
- 694 Lauvaux, T., Giron, C., Mazzolini, M., d'Aspremont, A., Duren, R., Cusworth, D., Shindell, D., and
695 Ciais, P.: Global assessment of oil and gas methane ultra-emitters, *Science*, 375, 557-561, 2022.
- 696 Leitner, S., Hood-Nowotny, R., and Watzinger, A.: Successive and automated stable isotope analysis of
697 CO₂, CH₄ and N₂O paving the way for unmanned aerial vehicle-based sampling, *Rapid*
698 *Communications in Mass Spectrometry*, 34, e8929, 2020.
- 699 Leitner, S., Feichtinger, W., Mayer, S., Mayer, F., Krompetz, D., Hood-Nowotny, R., and Watzinger, A.:
700 UAV-based sampling systems to analyse greenhouse gases and volatile organic compounds
701 encompassing compound-specific stable isotope analysis, *Atmospheric Measurement Techniques*,
702 16, 513-527, 2023.
- 703 Liu, Q., Wu, X., Wang, X., Jin, Z., Zhu, D., Meng, Q., Huang, S., Liu, J., and Fu, Q.: Carbon and
704 hydrogen isotopes of methane, ethane, and propane: A review of genetic identification of natural gas,
705 *Earth-Science Reviews*, 190, 247-272, 2019.
- 706 Liu, S.: Development of a UAV-based system to monitor air quality over an oil field, Montana Tech of
707 The University of Montana, 2018.
- 708 Liu, S., Yang, X., and Zhou, X.: Development of a low-cost UAV-based system for CH₄ monitoring
709 over oil fields, *Environmental Technology*, 42, 3154-3163, 10.1080/09593330.2020.1724199, 2021.
- 710 Lopez, M., Sherwood, O. A., Dlugokencky, E. J., Kessler, R., Giroux, L., and Worthy, D. E. J.: Isotopic
711 signatures of anthropogenic CH₄ sources in Alberta, Canada, *Atmospheric Environment*, 164, 280-
712 288, 2017.
- 713 Lu, X., Harris, S. J., Fisher, R. E., France, J. L., Nisbet, E. G., Lowry, D., Röckmann, T., van der Veen,
714 C., Menoud, M., Schwietzke, S., and Kelly, B. F. J.: Isotopic signatures of major methane sources in
715 the coal seam gas fields and adjacent agricultural districts, Queensland, Australia, *Atmos. Chem.*



- 716 Phys., 21, 10527-10555, 2021.
- 717 Malerba, M. E., de Kluyver, T., Wright, N., Schuster, L., and Macreadie, P. I.: Methane emissions from
718 agricultural ponds are underestimated in national greenhouse gas inventories, *Communications Earth
719 & Environment*, 3, 306, 2022.
- 720 McGowan, H. and Clark, A.: Identification of dust transport pathways from Lake Eyre, Australia using
721 Hysplit, *Atmospheric Environment*, 42, 6915-6925, 2008.
- 722 Menoud, M., van der Veen, C., Maazallahi, H., Hensen, A., Velzeboer, I., van den Bulk, P., Delre, A.,
723 Korben, P., Schwietzke, S., Ardelean, M., Calcan, A., Etiope, G., Baciu, C., Scheutz, C., Schmidt,
724 M., and Röckmann, T.: CH₄ isotopic signatures of emissions from oil and gas extraction sites in
725 Romania, *Elementa: Science of the Anthropocene*, 10, 2022.
- 726 Milkov, A. V., Schwietzke, S., Allen, G., Sherwood, O. A., and Etiope, G.: Using global isotopic data to
727 constrain the role of shale gas production in recent increases in atmospheric methane, *Scientific
728 Reports*, 10, 4199, 2020.
- 729 Minami, K. and Neue, H.-U.: Rice paddies as a methane source, *Climatic change*, 27, 13-26, 1994.
- 730 Montzka, S. A., Dlugokencky, E. J., and Butler, J. H.: Non-CO₂ greenhouse gases and climate
731 change, *Nature*, 476, 43-50, 2011.
- 732 Moreira, M., Sternberg, L., Martinelli, L., Victoria, R., Barbosa, E., Bonates, L., and Nepstad, D.:
733 Contribution of transpiration to forest ambient vapour based on isotopic measurements, *Global
734 Change Biology*, 3, 439-450, 1997.
- 735 National data: https://tjj.sc.gov.cn/scstjj/c111701/common_list.shtml, last
736 Global Monitoring Laboratory: <https://gml.noaa.gov/dv/data/>, last
737 HYSPLIT Trajectory Model: <https://www.ready.noaa.gov/hypub-bin/traject.pl>, last
- 738 Omara, M., Sullivan, M. R., Li, X., Subramanian, R., Robinson, A. L., and Presto, A. A.: Methane
739 emissions from conventional and unconventional natural gas production sites in the Marcellus Shale
740 Basin, *Environmental science & technology*, 50, 2099-2107, 2016.
- 741 Parnell, A. C., Phillips, D. L., Bearhop, S., Semmens, B. X., Ward, E. J., Moore, J. W., Jackson, A. L.,
742 Grey, J., Kelly, D. J., and Inger, R.: Bayesian stable isotope mixing models, *Environmetrics*, 24, 387-
743 399, 2013.
- 744 Pataki, D. E., Ehleringer, J. R., Flanagan, L. B., Yakir, D., Bowling, D. R., Still, C. J., Buchmann, N.,
745 Kaplan, J. O., and Berry, J. A.: The application and interpretation of Keeling plots in terrestrial
746 carbon cycle research, *Global Biogeochemical Cycles*, 17, 2003.
- 747 Peng, L., Ti, C., Yin, B., Dong, W., Li, M., Tao, L., and Yan, X.: Traceability of atmospheric ammonia
748 in a suburban area of the Beijing-Tianjin-Hebei region, *Science of The Total Environment*, 907,
749 167935, 2024.
- 750 Pereira, A. P. M. F., Rodrigues, L. A. d. C., Santos, E. A. d., Cardoso, T. A. d. O., and Cohen, S. C.:
751 CBRN events management and the use of the Hysplit model: an integrative literature review, *Saúde
752 em Debate*, 43, 925-938, 2019.
- 753 G2132-i Isotope Analyzer: https://www.picarro.com/environmental/products/g2132i_isotope_analyzer,
754 last
- 755 Rice, A. L., Butenhoff, C. L., Teama, D. G., Röger, F. H., Khalil, M. A. K., and Rasmussen, R. A.:
756 Atmospheric methane isotopic record favors fossil sources flat in 1980s and 1990s with recent
757 increase, *Proceedings of the National Academy of Sciences*, 113, 10791-10796, 2016.
- 758 Rigby, M., Montzka, S. A., Prinn, R. G., White, J. W., Young, D., O'doherty, S., Lunt, M. F., Ganesan,
759 A. L., Manning, A. J., and Simmonds, P. G.: Role of atmospheric oxidation in recent methane



- 760 growth, *Proceedings of the National Academy of Sciences*, 114, 5373-5377, 2017.
- 761 Saunio, M., Jackson, R. B., Bousquet, P., Poulter, B., and Canadell, J. G.: The growing role of
762 methane in anthropogenic climate change, *Environmental Research Letters*, 11, 120207, 2016a.
- 763 Saunio, M., Bousquet, P., Poulter, B., Peregon, A., Ciais, P., Canadell, J. G., Dlugokencky, E. J.,
764 Etiope, G., Bastviken, D., Houweling, S., Janssens-Maenhout, G., Tubiello, F. N., Castaldi, S.,
765 Jackson, R. B., Alexe, M., Arora, V. K., Beerling, D. J., Bergamaschi, P., Blake, D. R., Brailsford, G.,
766 Brovkin, V., Bruhwiler, L., Crevoisier, C., Crill, P., Covey, K., Curry, C., Frankenberg, C., Gedney,
767 N., Höglund-Isaksson, L., Ishizawa, M., Ito, A., Joos, F., Kim, H. S., Kleinen, T., Krummel, P.,
768 Lamarque, J. F., Langenfelds, R., Locatelli, R., Machida, T., Maksyutov, S., McDonald, K. C.,
769 Marshall, J., Melton, J. R., Morino, I., Naik, V., O'Doherty, S., Parmentier, F. J. W., Patra, P. K.,
770 Peng, C., Peng, S., Peters, G. P., Pison, I., Prigent, C., Prinn, R., Ramonet, M., Riley, W. J., Saito,
771 M., Santini, M., Schroeder, R., Simpson, I. J., Spahni, R., Steele, P., Takizawa, A., Thornton, B. F.,
772 Tian, H., Tohjima, Y., Viovy, N., Voulgarakis, A., van Weele, M., van der Werf, G. R., Weiss, R.,
773 Wiedinmyer, C., Wilton, D. J., Wiltshire, A., Worthy, D., Wunch, D., Xu, X., Yoshida, Y., Zhang, B.,
774 Zhang, Z., and Zhu, Q.: The global methane budget 2000–2012, *Earth Syst. Sci. Data*, 8, 697-751,
775 2016b.
- 776 Schoell, M.: The hydrogen and carbon isotopic composition of methane from natural gases of various
777 origins, *Geochimica et Cosmochimica Acta*, 44, 649-661, 1980.
- 778 Schwietzke, S., Sherwood, O. A., Bruhwiler, L. M. P., Miller, J. B., Etiope, G., Dlugokencky, E. J.,
779 Michel, S. E., Arling, V. A., Vaughn, B. H., White, J. W. C., and Tans, P. P.: Upward revision of
780 global fossil fuel methane emissions based on isotope database, *Nature*, 538, 88-91, 2016.
- 781 Shan, W., Yin, Y., Lu, H., and Liang, S.: A meteorological analysis of ozone episodes using HYSPLIT
782 model and surface data, *Atmospheric Research*, 93, 767-776, 2009.
- 783 Shaw, J. T., Shah, A., Yong, H., and Allen, G.: Methods for quantifying methane emissions using
784 unmanned aerial vehicles: A review, *Philosophical Transactions of the Royal Society A*, 379,
785 20200450, 2021.
- 786 Sherwood Lollar, B., Westgate, T., Ward, J., Slater, G., and Lacrampe-Couloume, G.: Abiogenic
787 formation of alkanes in the Earth's crust as a minor source for global hydrocarbon reservoirs, *Nature*,
788 416, 522-524, 2002.
- 789 2023 the statistical bulletin of national economic and social development of Sichuan province:
790 https://tjj.sc.gov.cn/scstjj/c111701/common_list.shtml, last
791 Scientific and technological paths and policy suggestions for reducing greenhouse gas emissions from
792 paddy fields in our province:
793 <https://nynct.sc.gov.cn/nynct/c110427/2021/9/3/2e13facab72e4608bb5ef0ea1aa345d7.shtml>, last
794 Skeie, R. B., Hodnebrog, Ø., and Myhre, G.: Trends in atmospheric methane concentrations since 1990
795 were driven and modified by anthropogenic emissions, *Communications Earth & Environment*, 4,
796 317, 2023.
- 797 Stein, A. F., Draxler, R. R., Rolph, G. D., Stunder, B. J. B., Cohen, M. D., and Ngan, F.: NOAA's
798 HYSPLIT Atmospheric Transport and Dispersion Modeling System, *Bulletin of the American
799 Meteorological Society*, 96, 2059-2077, 2015.
- 800 Sun, S., Ma, L., and Li, Z.: A Source-Level Estimation and Uncertainty Analysis of Methane Emission
801 in China's Oil and Natural Gas Sector, 2022.
- 802 Suzuki, Y.: Achieving food authenticity and traceability using an analytical method focusing on stable
803 isotope analysis, *Analytical Sciences*, 37, 189-199, 2021.

- 33



848 Zhu, G., Wang, Z., Dai, J., and Su, J.: Natural gas constituent and carbon isotopic composition in
849 petroliferous basins, China, *Journal of Asian Earth Sciences*, 80, 1-17, 2014.
850 Zou, Y.-R., Cai, Y., Zhang, C., Zhang, X., and Peng, P. a.: Variations of natural gas carbon isotope-type
851 curves and their interpretation – A case study, *Organic Geochemistry*, 38, 1398-1415, 2007.
852